Molecular Cancer Therapeutics

GC1118, an Anti-EGFR Antibody with a Distinct Binding Epitope and Superior Inhibitory Activity against High-Affinity EGFR Ligands

Yangmi Lim[1], Jiho Yoo[2], Min-Soo Kim[1], Minkyu Hur[1,3], Eun Hee Lee[1], Hyung-Suk Hur[1], Jae-Chul Lee[1], Shi-Nai Lee[1], Tae Wook Park[1], Kyuhyun Lee[1], Ki Hwan Chang[1], Kuglae Kim[2], YingJin Kang[2], Kwang-Won Hong[1], Se-Ho Kim[4], Yeon-Gil Kim[5], Yeup Yoon[6,7,8], Do-Hyun Nam[6,7,8,9], Heekyoung Yang[6,7,9], Dong Geon Kim[6,8], Hyun-Soo Cho[2], and Jonghwa Won[1]

Abstract

The EGFR-targeted monoclonal antibodies are a valid therapeutic strategy for patients with metastatic colorectal cancer (mCRC). However, only a small subset of mCRC patients has therapeutic benefits and there are high demands for EGFR therapeutics with a broader patient pool and more potent efficacy. In this study, we report GC1118 exhibiting a different character in terms of binding epitope, affinity, mode of action, and efficacy from other anti-EGFR antibodies. Structural analysis of the EGFR–GC1118 crystal complex revealed that GC1118 recognizes linear, discrete N-terminal epitopes of domain III of EGFR, critical for EGF binding but not overlapping with those of other EGFR-targeted antibodies. GC1118 exhibited superior inhibitory activity against high-affinity EGFR ligands in terms of EGFR binding, triggering EGFR signaling, and proliferation compared with cetuximab and panitumumab. EGFR signaling driven by low-affinity ligands, on the contrary, was well inhibited by all the antibodies tested. GC1118 demonstrated robust antitumor activity in tumor xenografts with elevated expression of high-affinity ligands *in vivo*, whereas cetuximab did not. Considering the significant role of high-affinity EGFR ligands in modulating tumor microenvironment and inducing resistance to various cancer therapeutics, our study suggests a potential therapeutic advantage of GC1118 in terms of efficacy and a range of benefited patient pool.
Mol Cancer Ther; 15(2); 251–63. ©2015 AACR.

Introduction

EGFR, a member of the ErbB or HER family of receptors, regulates various cellular processes including proliferation, differentiation, migration, and invasion (1). The dysregulation of EGFR has been observed in a wide range of cancers (2, 3) and implicated in tumor progression and resistance to radiation-induced cell death (4).

Enhanced EGFR ligand expression and an autocrine or paracrine EGFR circuit are the main mechanisms in cancer development and progression (5). The EGFR ligand family is comprised of seven transmembrane precursor proteins whose expression and processing is tightly regulated. These ligands can be classified on the basis of their affinity for EGFR. EGF, β-cellulin (BTC), heparin-binding EGF-like growth factor (HB-EGF), and TGFα are high-affinity ligands with binding affinity (K_D) of 0.6 to 9.2 nmol/L, whereas amphiregulin (AREG), epiregulin (EREG), and epigen (EPI) are considered low-affinity ligands with K_D of 350 nmol/L to 2.8 μmol/L (6, 7). EGFR ligands exhibit different signaling intensities, durations, and trafficking, resulting in differential EGFR signaling and physiologic consequences (8–10). AREG and EREG are EGFR ligands that are predominantly expressed in CRC cell lines (11). mCRC patients with a higher gene expression of EREG and AREG prior to treatment tend to have better disease control by cetuximab than low expressers (12). On the other hand, mCRC patients with disease progression have elevated TGFα (13). An increased expression of high-affinity ligands, such as TGFα and HB-EGF, was also observed in a mouse colorectal cancer model with acquired resistance to cetuximab (14). An elevated level of TGFα or HB-EGF has been observed in other cancers, including advanced ovarian cancer, breast cancer (15–17), and lung cancer (18), and is associated with worse clinical survival.

[1]MOGAM Biotechnology Institute, Yongin, Gyeonggi-do, Republic of Korea. [2]Department of Systems Biology, College of Life Science and Biotechnology, Yonsei University, Seoul, Republic of Korea. [3]Graduate School of Medicine, Korea University College of Medicine, Korea University, Seoul, Republic of Korea. [4]University-Industry Cooperation Foundation, and Department of Systems Immunology, College of Biomedical Science, Kangwon National University, Chuncheon, Kangwon-Do, Republic of Korea. [5]Pohang Accelerator Laboratory, Pohang University of Science and Technology, Pohang, Kyungbuk, Republic of Korea. [6]Institute for Refractory Cancer Research, Samsung Medical Center, Seoul, Republic of Korea. [7]Samsung Biomedical Research Institute, Samsung Medical Center, Seoul, Republic of Korea. [8]Department of Health Sciences and Technology, SAIHST, Sungkyunkwan University, Seoul, Republic of Korea. [9]Samsung Medical Center, School of Medicine, Sungkyunkwan University, Seoul, Republic of Korea.

Note: Supplementary data for this article are available at Molecular Cancer Therapeutics Online (http://mct.aacrjournals.org/).

Y. Lim and J. Yoo contributed equally to this article.

Corresponding Authors: Jonghwa Won, MOGAM Biotechnology Institute, 341 Bojeong-dong, Giheung-gu, Yongin, Gyeonggi-do 446-799, Republic of Korea (South). Phone: 8231-260-9811; Fax: 8231-260-9808; E-mail: agnes@mogam.re.kr; and Hyun-Soo Cho, E-mail: hscho8@yonsei.ac.kr

doi: 10.1158/1535-7163.MCT-15-0679

Structural studies of the EGF–EGFR complex depict the process of EGFR activation after ligand binding (19–22), which triggers a conformational change in EGFR from a tethered form to an open form. EGFR-targeted antibodies on the market or under development differ in their isotype, binding affinity, and mechanism of EGFR binding, and show different characteristics (23, 24). Recently, mixtures of antibodies targeting nonoverlapping epitopes on EGFR (Sym004 and MM-151) were developed and reported to have enhanced inhibitory activity on EGFR signaling and tumor progression (25, 26).

In this study, we disclose the novel anti-EGFR antibody GC1118 with a distinct binding epitope and efficacy. The superior inhibitory activity of GC1118 on high-affinity EGFR ligands, to which current clinical antibodies show restricted inhibitory activity, reflects the potential therapeutic advantage of GC1118 in treating cancer patients where high-affinity EGFR ligands are implicated in tumor progression, metastasis, and resistance to current cancer therapeutics.

Materials and Methods

Expression and purification of soluble EGFR and GC1118 Fab

The extracellular domain of EGFR encompassing domains I–IV (sEGFR) was expressed using a baculovirus expression system in *Spodoptera frugiperda* (Sf9) cells. After adjusting the pH of the expression media to 7.5, the medium was applied to an NHS-activated HP column (GE Healthcare) coupled with GC1118 IgG. sEGFR was eluted using an elution buffer (20 mmol/L Na-citrate pH 3.0, 100 mmol/L NaCl) after washing the column with a wash buffer (20 mmol/L Tris-HCl pH 7.5, 100 mmol/L NaCl). The eluted sEGFR was applied to a HiLoad 16/600 Superdex200 PG column (GE Healthcare) for size exclusion chromatography (SEC) purification with the SEC buffer (20 mmol/L Tris-HCl pH7.5, 100 mmol/L NaCl).

The Fab fragment of GC1118 was generated by digestion with a papain. GC1118 was incubated with a papain (1:50 w/w) in 1 mmol/L DTT at 37°C for 1 hour and the reaction was stopped with 20 mmol/L iodoacetamide. To remove the Fc fragment, papain-treated solution was mixed with a Protein A resin for 1 hour at 4°C. A flow-through including Fab proteins was collected. These fractions were further purified by a gel filtration (HiLoad 16/600 Superdex200 PG column, GE Healthcare) and confirmed with a SDS-PAGE.

The purified sEGFR and the Fab fragment of GC1118 were mixed at a 1:2 molar ratio and incubated for 1 hour at 4°C. The sEGFR–GC1118 Fab fragment complex was purified using a HiLoad 16/600 Superdex200 PG column with the SEC buffer. The complex was confirmed by SDS-PAGE and concentrated to 15 mg/mL for crystallization.

Crystallization, data collection, and structure determination

Optimized crystallization condition for sEGFR–GC1118 complex was 0.1 mol/L ammonium sulfate, 0.1 mol/L Na-acetate (pH 4.6), and 25% PEG4000. In the initial crystallization screening of the sEGFR–GC1118 complex, a microbatch method was used with commercial crystal screening kits (Hampton Research). Equal volumes of sEGFR/GC1118 solution and crystallization buffer were mixed in microbatch plates and incubated for 1 week at 13°C.

For cryo protection, 15% ethylene glycol was added to the reservoir buffer before the X-ray diffraction experiments. Data were harvested by the Spring-8 beamline BL26B1. The X-ray diffraction data of the sEGFR–GC1118 complex were processed with HKL2000 (27). The sEGFR–GC1118 complex structure was determined by the molecular replacement method with Molrep in CCP4 suite using the sEGFR structure and Fab structure, respectively, from sEGFR–cetuximab complex structure (PDB ID: 1YY9) as a search model (28, 29). First, the sEGFR structure was used for molecular replacement. The found solution structure for sEGFR was fixed and then the Fab structure of cetuximab was used for second round of molecular replacement. One sEGFR–GC1118 Fab complex was found in asymmetry unit. Coot and Refmac5 were used for model building and refinement (30, 31). ArealMol and Sc program in CCP4 package were used to calculate buried surface area (BSA) and shape complementarity coefficient (Sc; ref. 29). The Pymol program was used for figure drawing and superposition of the complex structures of GC1118, cetuximab, and matuzumab. The statistics of the data collection and refinement are shown in Supplementary Table S1. The sEGFR–GC1118 complex structure is deposited in PDB (PDB ID: 4UV7).

Cell lines

Colorectal cancer cell lines (C2bbe1, HCT8, HCT15, LS174T, and LoVo) were obtained from ATCC from 2012 to 2014. The cell lines were maintained in DMEM or RPMI with 10% FBS. All cell lines were tested for mycoplasma contamination with MycoAlert PLUS Mycoplasma Detection Kit from Lonza. The cells were expanded, cryopreserved, and used within 6 months after resuscitation. No authentication was done by the authors.

Antibodies and reagents

Anti-pEGFR, anti-EGFR, anti-pERK, anti-ERK, anti-pAkt, and anti-Akt were purchased from Cell Signaling Technology. HB-EGF, TGFα, BTC, EREG, and AREG were purchased from R&D Systems. EGF was purchased from BD Biosciences. Horseradish peroxidase (HRP)-conjugated anti-mouse and anti-rabbit antibodies were purchased from Invitrogen. Cetuximab (Erbitux) was from Merck.

Flow cytometry–based EGFR-binding analysis

Colorectal cancer cells were preincubated with cetuximab (Merck) or GC1118 for 2 hours at 4°C and treated with various concentrations of ligands for 10 minutes at 37°C. After two washes with FACS buffer, the cells were incubated with 0.5 μg/mL of goat anti-human IgG-PE (Sigma) for 30 minutes at 4°C, washed twice with FACS buffer, and analyzed using a FACSCalibur. The final analysis and graphical output were generated using FlowJo (TreeStar) and GraphPad Prism 5.01 (GraphPad Software).

Immunoblotting

The cells were lysed using cell lysis buffer (Cell Signaling Technology) containing a protease and phosphatase inhibitor cocktail (Pierce), and clarified by centrifugation. The cell lysates (20 μg/lane) were resolved on SDS-PAGE gels and transferred to nitrocellulose membranes. After incubation with protein-free T20 blocking buffer (Pierce) for 1 hour, the membranes were incubated with primary antibody (1:2,000) overnight at 4°C and then incubated with 1:20,000 HRP-labeled secondary antibodies (Invitrogen) for 1 hour at room temperature. The protein signal was detected using an ECL Prime Western Blotting Detection Reagent (GE Healthcare).

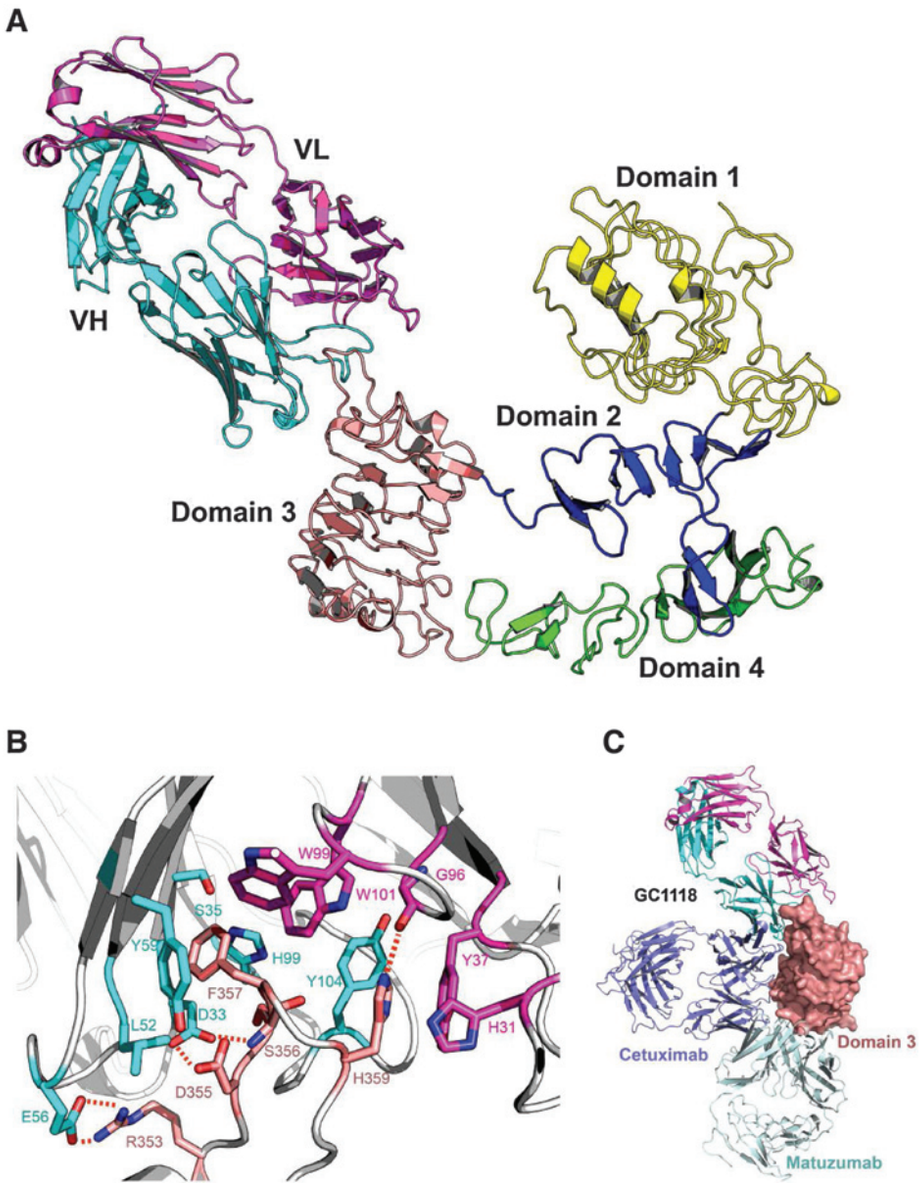

Figure 1.
Complex structure of sEGFR with the Fab fragment of GC1118. A, a ribbon diagram of the complex structure of sEGFR and the Fab fragment of GC1118. Each domain of sEGFR is shown in a different color (domain 1, yellow; domain 2, blue; domain 3, salmon; domain 4, green). The heavy chain and light chain of GC1118 are colored cyan and magenta, respectively. GC1118 binds to domain III of sEGFR in a tethered conformation. B, a close-up view of the GC1118 Fab–sEGFR interface. The heavy chain residues (cyan sticks and numbers) and light chain residues (magenta sticks and numbers) of GC1118 and the epitopes of sEGFR (salmon sticks and numbers) are labeled. C, the comparison of the binding modes of three antibodies (cetuximab, GC1118, and matuzumab) to domain III of sEGFR. The domain III of sEGFR is represented as a surface model. The Fab fragments of GC1118, cetuximab, and matuzumab are shown as cyan (VH)/magenta (VL), slate blue, and light blue color, respectively.

Ligand-induced proliferation and inhibition assay

Cell proliferation was measured using the CellTiter 96 Aqueous One solution Reagent (Promega) according to the manufacturer's instructions. The cells were plated into 96-well plates at a density of 2,500 to 7,000 cells per well and grown in DMEM or RPMI with 10% FBS. After 18 hours, the medium was completely changed to serum-free medium, followed by the addition of the antibody and EGFR ligands, and incubated for 3 days. MTS solution was added, and the proliferation level was determined using a microplate reader (VersaMax, Molecular Devices).

Tumor xenograft mouse model

Animal housing, handling, and all of the procedures involving mice were approved by the Institutional Animal Care and Use Committee of Green Cross Corp and MOGAM Biotechnology Institute (Approval number GC13-101A). Nude mice, 7 to 8 weeks of age, were subcutaneously injected with the 0.5–1 $\times$ 10^7 cells of colorectal cancer cell lines. Cohorts of 10 mice for each group were injected with colorectal cancer cells and observed until the tumor volume reached 100 to 200 mm^3. At that time, the mice were randomly assigned to a treatment group and treated with GC1118 or cetuximab at 1 mg/mouse twice a week for 5 weeks. The vehicle group received PBS. Tumor size was measured during the treatment period.

Measurement of the EGFR ligands in cell lines and tumor xenografts

The cells were seeded on a 6-well plate (1×10^5 cells/well) and incubated for 72 hours. The ligands released into the culture supernatant were assayed using ELISA. The human EGF, HB-EGF,

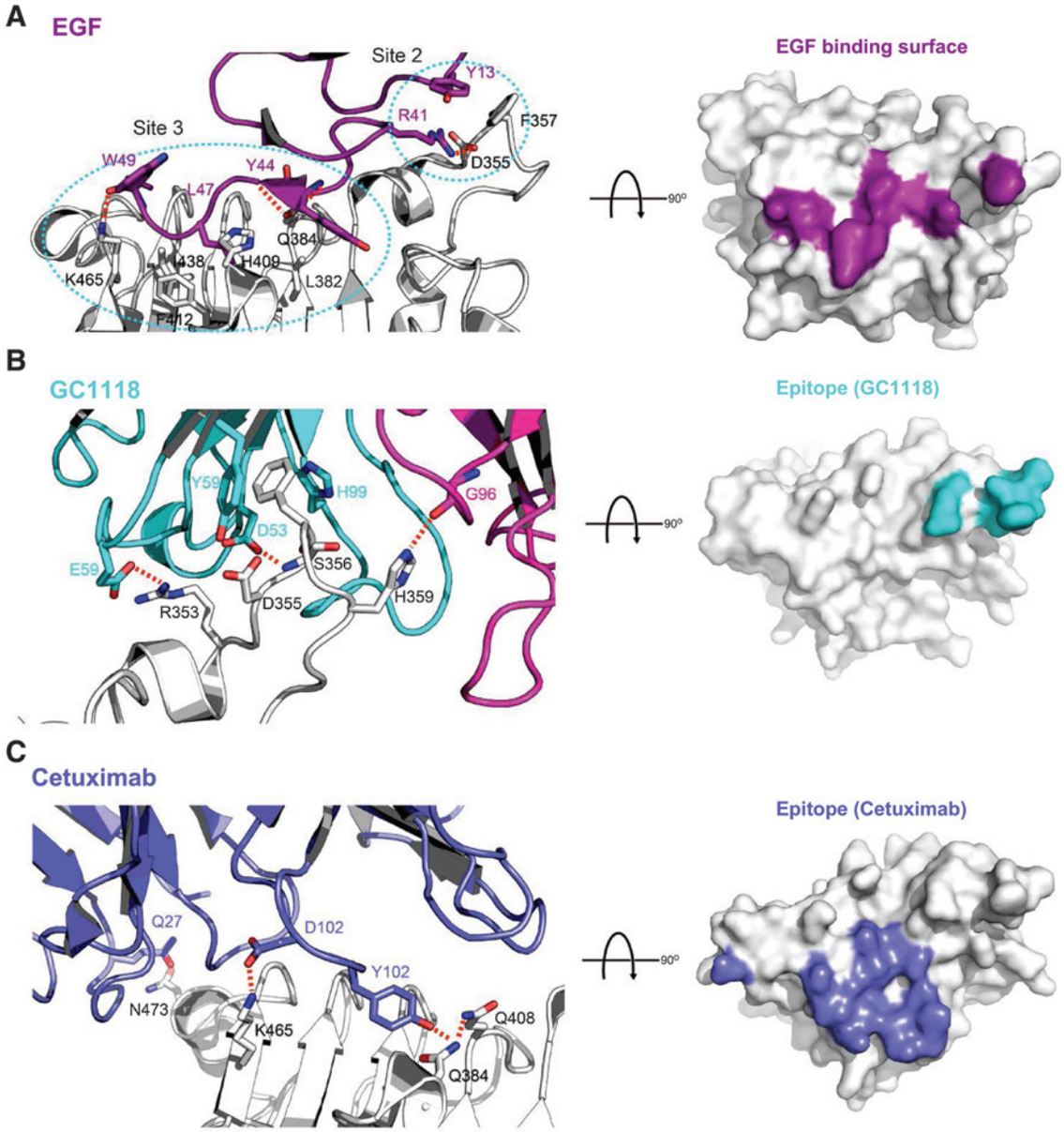

Figure 2.
Comparison of the EGFR-binding modes of EGF, GC1118, and cetuximab. sEGFR/EGF (PDB ID: 1IVO; A), sEGFR/GC1118 (B), and sEGFR/cetuximab (PDB ID: 1YY9; C) complex structures are represented. On the left side, domain III of sEGFR is depicted in gray. EGF, GC1118 VH/VL, and cetuximab are in purple, cyan/magenta, and slate blue, respectively. The binding residues of EGF, epitopes of GC1118, and cetuximab are labeled in their corresponding structure colors. On the right side, the binding regions of EGF and binding epitopes of GC1118 and cetuximab on domain III of sEGFR are colored as purple, cyan, and slate blue, respectively. This view is rotated 90° about a horizontal axis of each left complex structure.

TGFα, BTC, AREG ELISA kits purchased from Ray Biotech, Inc., and the human EREG ELISA kits purchased from USCN Life Science Inc. were used for the quantitative determination of the EGFR ligand expression levels.

The tumor samples were isolated when the tumor xenografts reached 200 mm^3. The tumor xenografts were extracted in 1 mL of lysis buffer (Cell Signaling Technology), homogenized, and used for ELISA at a concentration of 50 μg per well.

Results

The complex structure of the extracellular domain of EGFR and GC1118

GC1118 is a fully human antibody whose generation and affinity maturation process from the original mouse anti-EGFR antibody A13 was published previously (32, 33). To analyze the binding mode and predict the inactivation mechanism of EGFR

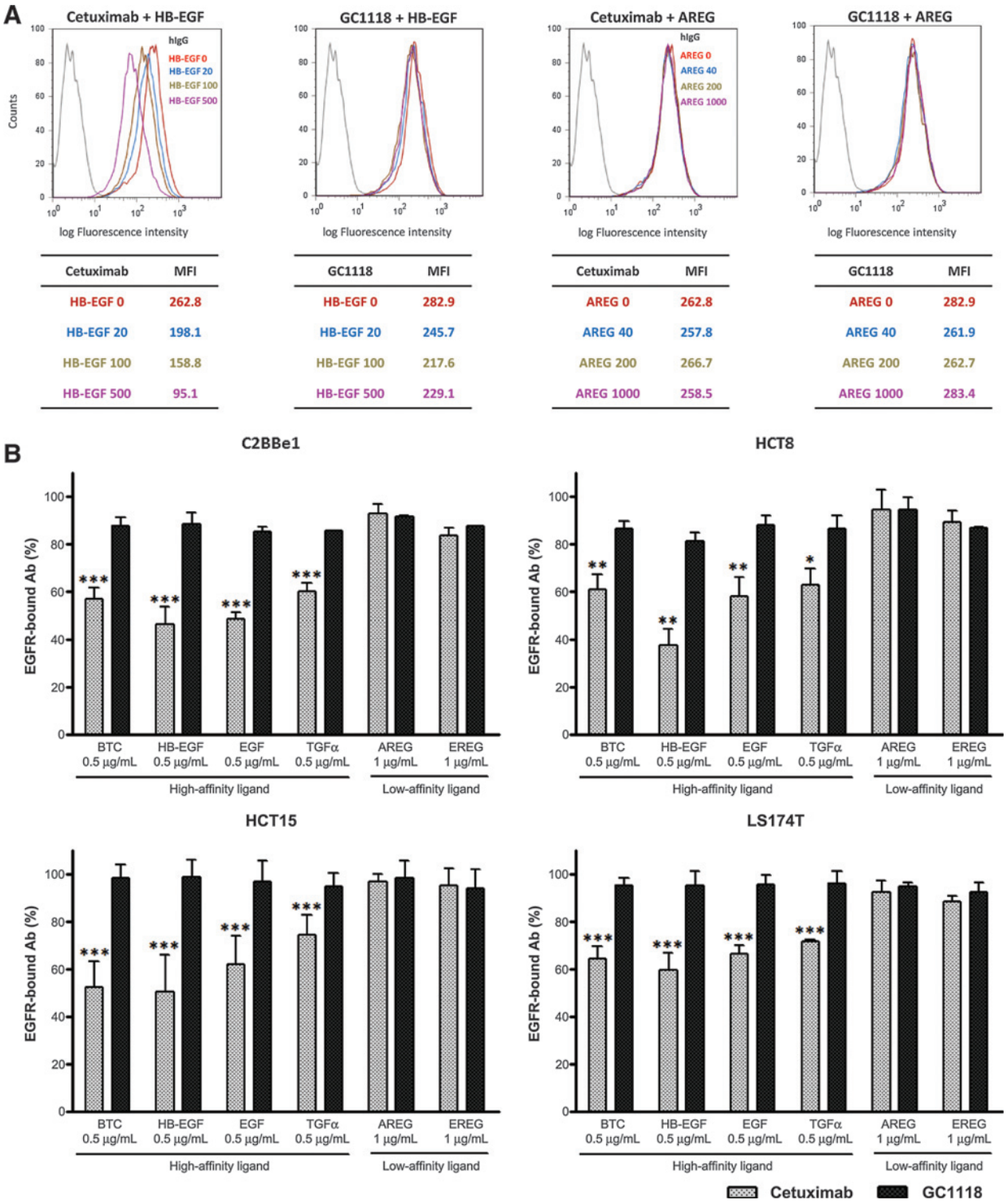

Figure 3.
The EGFR–GC1118 interaction is not disrupted by excess amounts of high- or low-affinity EGFR ligands. A, representative FACS analysis showing the competitive binding inhibition of cetuximab–EGFR and the GC1118–EGFR interaction with excess amounts of EGFR ligands. HCT8 cell lines were preincubated with 0.1 μg/mL of cetuximab or GC1118 for 2 hours prior to the addition of HB-EGF (20–500 ng/mL) or AREG (40–1000 ng/mL) for 10 minutes. Antibody binding to EGFR was assessed by measuring the fluorescence intensity using flow cytometry. B, the indicated colon cancer cell lines were preincubated with 0.1 μg/mL of cetuximab or GC1118 for 2 hours prior to the addition of EGFR ligands for 10 minutes (EGF, HB-EGF, BTC, and TGFα, 500 ng/mL; AREG and EREG, 1 μg/mL). The gray and black bars indicate the relative percentage of cetuximab and GC1118, respectively, bound to EGFR in the presence of competing ligands compared with bound antibodies in the absence of blocking ligands. Antibody binding to EGFR was assessed by measuring the fluorescence intensity using flow cytometry. The results are expressed as the percent average of EGFR-bound antibody ±SE of triplicate experiments. The difference between the GC1118 group and cetuximab group is significant (two-way ANOVA; *, $P < 0.5$; **, $P < 0.01$; and ***, $P < 0.001$). Ab, antibody.

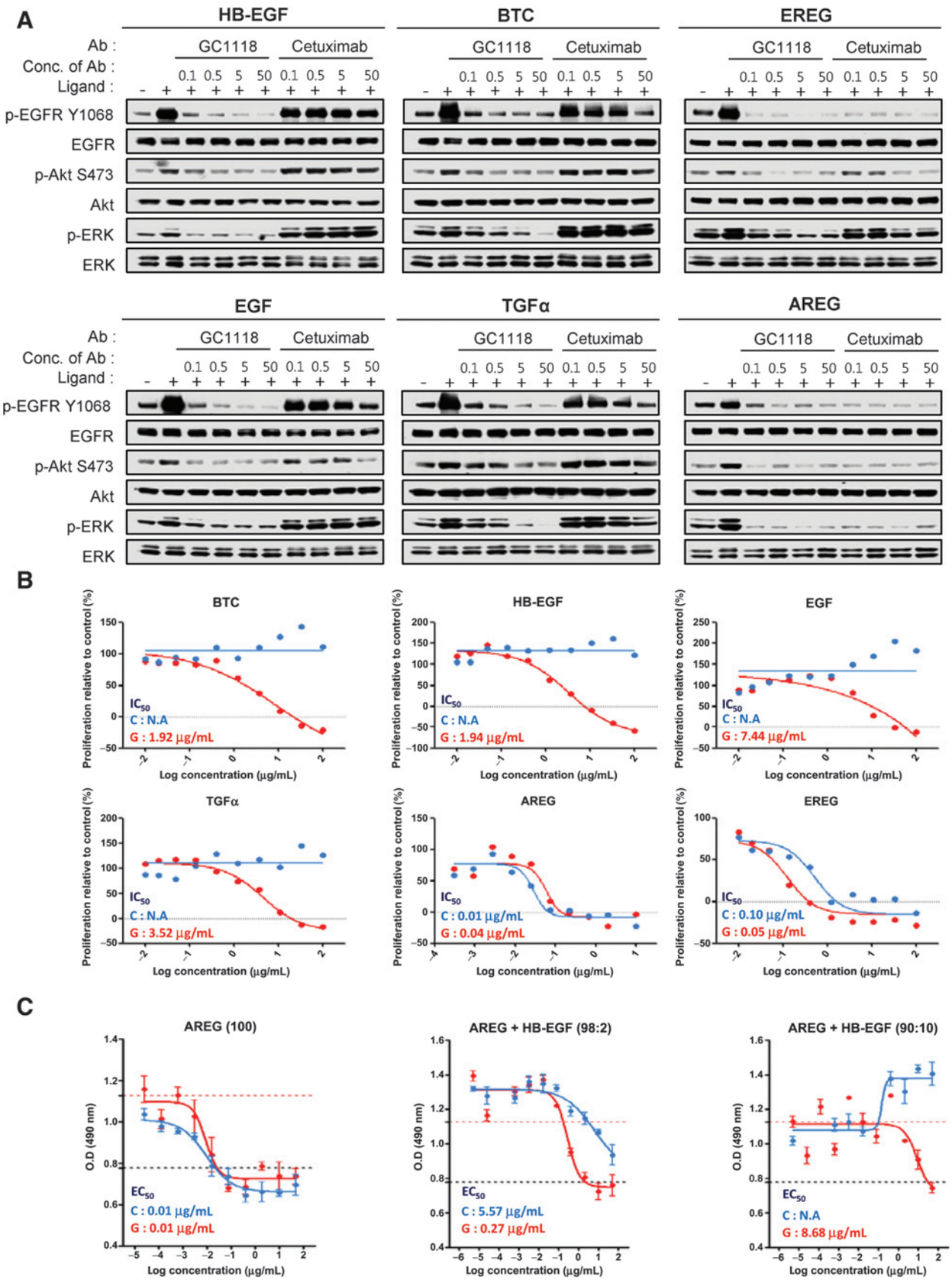

upon GC1118 binding, we determined a sEGFR–GC1118 Fab complex structure, using X-ray crystallography. A sEGFR–GC1118 Fab complex was purified by SEC and diffracted at 1.9 Å resolutions. Molecular replacement was applied to solve the complex structure of the sEGFR–GC1118 Fab by using reported structures of tethered sEGFR–cetuximab Fab complex. A refined sEGFR–GC1118 Fab complex structure at 2.1 Å resolution shows that one sEGFR–GC1118 Fab complex molecule is located in the asymmetry unit. Data collections and refinement statistics are summarized in Supplementary Table S1. EGFR in complex with GC1118 was found in a tethered form, where domain 2 interacts with domain 4. This result suggests that GC1118 inhibits the binding of ligands to EGFR and keeps EGFR in the tethered form (Fig. 1).

The complex structure revealed that GC1118 binds to a protruding loop in domain III of EGFR (amino acids R353-H359; Fig. 1A). Calculated BSA of sEGFR by GC1118 is a 649.35 $Å^2$. This is a smaller area than cetuximab (882 $Å^2$) and matuzumab (758 $Å^2$) because of a different epitope position in a domain III of EGFR. We also calculated Sc of sEGFR–GC1118 complex. It is 0.803, which is higher than cetuximab (0.71), matuzumab (0.62), and observed Sc of antigen/antibody (0.62–0.68) typically. This means that GC1118 fits to their epitope in sEGFR better than cetuximab and matuzumab.

F357 of EGFR is located at the tip of this loop and forms hydrophobic interactions with both V_H and V_L of GC1118 (Y59 and H99 of V_H and W99 and W101 of V_L). EGFR H359 forms a hydrogen bond with the backbone of G96 of the light chain (V_L G96) as well as hydrophobic interactions with V_H Y104 and V_L Y37. The nitrogen of EGFR S356 interacts with GC1118 through a hydrogen bond with of V_H D33. D355 forms a hydrogen bond with the side chain of V_H Y59 and van der Waals interactions with V_H L52. R353 forms an ionic interaction with the side chain of V_H E56 (Fig. 1B).

The GC1118–EGFR complex structure was superimposed with those of cetuximab and matuzumab based on previously published literature (34, 35). The epitopes of those three antibodies are all located in domain III of EGFR, but their binding patterns are quite different. While the binding epitopes of cetuximab are widely dispersed in domain III, those of matuzumab and GC1118 are on the linear discrete sequences (Fig. 1C; refs. 34, 35). GC1118 and matuzumab recognize the loop (from R353 to H359) located in the N-terminus and a short loop (from K454 to T464) in the C-terminus of domain III, respectively (Fig. 1C; refs. 34, 35). While the binding epitopes of cetuximab and GC1118 overlap with the EGF-binding sites, the epitope of matuzumab is located far from the EGF-binding site (21, 34, 35). Matuzumab does not inhibit EGF binding to EGFR but prevents the conformational change required for dimerization (35). Our data and previous reports support the conclusion that both GC1118 and cetuximab maintain EGFR in the tethered conformation and block EGF binding to EGFR and subsequent EGFR dimerization (34).

Comparison of the EGFR-binding sites of EGF, cetuximab, and GC1118

The crystal structure of EGF and its receptor revealed that EGF interacts with EGFR through three interfaces, one site on domain I and two sites on domain III of EGFR, namely site 2 and site 3 (Fig. 2A; ref. 21). Site 2 encompasses residues 350–357 and has two important interactions: a hydrophobic interaction formed between the aromatic residue of EGF Y13 and EGFR F357, and a salt bridge between EGF R41 (100% conserved throughout the ligands) and EGFR D355 (Fig. 2A). These two interactions involving R41 and Y13 of EGF were found to be critical determinants for receptor binding (21, 36, 37). Site 3 has two distinct interactions, a hydrophobic and hydrophilic interaction. The hydrophobic pocket consisting of L382, F412, and I438 in EGFR forms an interaction with EGF L47, and several residues on the receptor, such as Q384 and K465, form a hydrogen bond with the ligand (21).

The binding epitopes of GC1118 and cetuximab overlap with the EGF-binding site on domain III (Fig. 2). The epitope of GC1118 primarily resides on site 2 encompassing residues 350–357, whereas the epitopes of cetuximab are dispersed on site 3 including Q384-N473 (Figs. 1B and 2B and C). The epitopes of GC1118 (R353-H359) fully overlap with site 2, which is the critical binding site of EGF to EGFR. The interaction between GC1118 Y59 (on HCDR2 of GC1118) and EGFR D355 would block a salt bridge between EGF R41 and EGFR D355, one of the critical sites for the EGF–EGFR interaction. In addition, H99 on HCDR3 and W99 and W101 on the LCDR3 of GC1118 thoroughly hinder the hydrophobic interaction between EGFR F357 and EGF Y13. On the other hand, the binding epitopes of cetuximab are largely superimposed with site 3. Y102 on the HCDR3 of cetuximab protrudes into the hydrophobic pocket of site 3, where EGF L47 (L48 in TGFα) interacts with EGFR Q384 and EGFR Q408 through hydrogen bonds (34, 38).

GC1118 efficiently blocks the binding of high- as well as low-affinity ligands to EGFR

GC1118 has binding affinity of 0.16 nmol/L (K_D) to EGFR, compared with cetuximab, which has a K_D of 4.5 nmol/L (Supplementary Fig. S1; Supplementary Table S2). Different binding affinities and binding modes of GC1118 could lead to differential effects on ligand competition for EGFR. To test this hypothesis, GC1118 was labeled with a fluorescent dye, and the level of EGFR-bound GC1118 in cancer cells was measured using flow cytometry. Increasing concentrations of EGFR ligands were introduced to determine the binding inhibitory effect of GC1118, where

Figure 4.

GC1118 blocks EGFR high- and low-affinity ligand-induced EGFR signaling and proliferation. A, HCT8 cells were serum starved for 18 hours, treated with 0.1 to 50 μg/mL GC1118 or cetuximab for 2 hours, and stimulated with EGFR ligands (EGF, HB-EGF, BTC, and TGFα, 250 ng/mL; AREG, 300 ng/mL; EREG, 500 ng/mL). pEGFR, pAKT, pERK, EGFR, AKT, and ERK expression levels were analyzed by Western blotting. B, HCT8 cells were serum starved for 18 hours, treated with ligands (EGF and HB-EGF, 50 ng/mL; BTC, 100 ng/mL; TGFα, 200 ng/mL; AREG and EREG, 300 ng/mL) and various amounts of GC1118 or cetuximab (0.005–100 μg/mL in high-affinity ligand-induced proliferation, 5 pg/mL–10 μg/mL in low-affinity ligand-induced proliferation) for three days. Cell proliferation was analyzed using an MTS assay. Red lines represent GC1118-treated cells and blue lines indicate cetuximab-treated cells. C, HCT8 cells were serum starved for 18 hours, treated with various ratios of ligands and 25 pg/mL to 50 μg/mL of GC1118 or cetuximab for three days. Cell proliferation was analyzed using an MTS assay. AREG (100), 200 ng/mL of AREG only; AREG+HB-EGF (98:2), mixtures of AREG and HB-EGF with a molar ratio of 98:2 (196 ng/mL AREG, 8.4 ng/mL HB-EGF), AREG+HB-EGF (90:10), mixtures of AREG and HB-EGF with a molar ratio of 90:10 (180 ng/mL AREG, 42 ng/mL HB-EGF). Red lines represent GC1118-treated cells and blue lines indicate cetuximab-treated cells.

GC1118 displacement leads to decreased fluorescent intensity and a binding peak shift to the left.

Colorectal cancer cell lines were preincubated for 2 hours with 0.1 μg/mL of GC1118 or cetuximab (which is 0.667 nmol/L of GC1118 and 0.658 nmol/L of cetuximab), the antibody concentration where most of EGFRs are occupied by antibodies and, therefore, both antibodies show a similar binding intensity. The cells were washed and incubated with various concentrations of EGFR ligands for 10 minutes. The GC1118 or cetuximab bound to EGFR on the colorectal cancer cells was detected using a flow cytometer. The EGFR-bound antibody level in each setting is marked as a relative percentage by setting the EGFR-bound antibody level in the absence of competing ligands as 100%. The relative percentages of both of the EGFR-bound cetuximab and GC1118 were not reduced by increasing concentrations of AREG and EREG (Fig. 3). Even 136- to 277-fold excess molar ratios of low-affinity ligands (1 μg/mL of AREG and EREG is 91 and 185 nmol/L, respectively) could displace neither GC1118 nor cetuximab from EGFR (Fig. 3 and Supplementary Fig. S2), indicating that low-affinity ligands are well blocked from binding to EGFR by these two antibodies. The fraction of EGFR-bound cetuximab decreased as the concentration of high-affinity ligands increased, while GC1118 maintained its binding status to EGFR in the presence of up to 32- to 125-fold excess amounts of high-affinity ligands (0.5 μg/mL of HB-EGF, BTC, EGF, and TGFα are 21.7 nmol/L, 33.3 nmol/L, 83.3 nmol/L, and 83.3 nmol/L, respectively; Fig. 3 and Supplementary Fig. S2). Among the high-affinity ligands, cetuximab appeared to be easily displaced by HB-EGF, in which 20% and 40% to 60% of cetuximab was detached from EGFR with a 1.3- and 32-fold excess molar ratio of HB-EGF, respectively. These results indicate that GC1118 potently blocks the interaction of EGFR with a broad range of ligands.

GC1118 exhibits a potent inhibition on high-affinity EGFR ligand–induced signaling and proliferation

The binding of EGF ligands to EGFR activates the tyrosine kinase activity of the receptor (2). Tyrosine 1068 (Y1068) of EGFR is one of the major phosphorylation sites that allow Grb2 binding and activation of the MAPK signaling pathway (39). To determine the inhibitory activities of GC1118 on EGFR signaling, colorectal cancer cells were induced with EGFR ligands in the presence or absence of GC1118 or cetuximab, and the phosphorylation status of key EGFR signaling molecules was evaluated (Fig. 4A). GC1118 completely inhibited the high-affinity EGFR ligand–induced Y1068 phosphorylation of EGFR starting from 0.1 μg/mL, whereas a complete inhibition was observed only at 50 μg/mL of cetuximab (Fig. 4A). For HB-EGF–induced Y1068 phosphorylation, up to 50 μg/mL of cetuximab showed no inhibition. Both antibodies efficiently blocked the low-affinity EGFR ligand (EREG, AREG)-induced Y1068 phosphorylation in a dose-dependent manner (Fig. 4A). A potent inhibitory effect of GC1118 on high-affinity EGFR ligand–induced signaling was more pronounced for the EGFR downstream signaling molecules, including Akt and Erk (Fig. 4A).

To evaluate the inhibitory activity of GC1118 on EGFR ligand–induced proliferation, HCT8 cell line was treated with EGFR ligands in the presence of antibodies. GC1118 was capable of potently inhibiting both high- and low-affinity EGFR ligand-driven cell proliferation, whereas the inhibitory activities of cetuximab were restricted to only low-affinity EGFR ligand–driven cell proliferation (Fig. 4B).

EREG and AREG are predominant EGFR ligands expressed in colorectal cancer and only a small fraction of high-affinity ligands are expressed (12). To simulate the impact of high-affinity ligands on antibody efficacy in colorectal cancer patients, the HCT8 cell line was treated with increasing concentrations of HB-EGF, and the inhibitory activities of the antibodies on cell growth were evaluated. Both antibodies efficiently inhibited AREG-induced proliferation with an EC_{50} of 0.01 μg/mL (0.067 nmol/L); however, as the concentration of HB-EGF increased (molar ratio of AREG: HB-EGF = 98:2 and 90:10), the inhibitory activity of cetuximab on proliferation reduced gradually and finally disappeared (Fig. 4C). Even a small fraction of HB-EGF (10% in the total ligand pool) completely blocked the inhibitory activity of cetuximab. On the other hand, GC1118 maintained its inhibitory activity, although it decreased slightly, with an EC_{50} of 0.27 and 8.68 μg/mL in the presence of HB-EGF at a molar ratio of 2% and 10%, respectively (Fig. 4C).

GC1118 shows superior antitumor activity in colorectal cancer cells secreting a high level of high-affinity EGFR ligands

To investigate a link between the superior inhibitory effect of GC1118 and the expression of EGFR ligands, we examined the *in vitro* and *in vivo* EGFR ligand expression profiles of various colorectal cancer cell lines: LS174T, HCT15, LoVo, HCT8, LS513, and SW48. AREG and EREG are the predominant EGFR ligands expressed in these cells as reported by others when cultured *in vitro* (Fig. 5A; ref. 11). GC1118 and cetuximab exerted a similar proliferation inhibitory effect in the absence of extraneously added EGFR ligands (data not shown).

The EGFR ligand expression profile in tumor xenografts was quite different from that observed in *in vitro* culture. Tumor xenografts of 200 mm^3 were isolated and used for the EGFR ligand analysis. The expression of high-affinity ligands appeared to be induced and more prevalent in the tumor xenografts of LS174T, HCT15, LoVo, and HCT8 than in cells in *in vitro* culture (Fig. 5B). The LS513 and SW48 tumors maintained their ligand expression pattern exhibited when cultured *in vitro*, where AREG and EREG were the predominant EGFR ligands (Fig. 5B).

To test antitumor efficacy, mice with tumors of 200 mm^3 were randomly assigned and treated with each antibody twice a week. The GC1118-treated group showed significant tumor progression retardation compared with the cetuximab-treated group in LS174T, HCT15, HCT8, and LoVo xenograft models, which predominantly expressed high-affinity ligands (Fig. 5C). In contrast, both GC1118 and cetuximab effectively suppressed the tumor growth of LS513 and SW48 xenografts, which show a relatively low expression of high-affinity ligands (Fig. 5B and C). These results support the conclusion that cetuximab has limited inhibitory activity on tumor xenografts with an elevated level of high-affinity ligand expression. On the other hand, GC1118 has potent antitumor efficacy in colorectal cancer xenografts regardless of the EGFR ligands and may show efficacy on a broader colorectal cancer patient pool compared with cetuximab.

Panitumumab, showing a higher binding affinity to EGFR compared with cetuximab, also failed to exhibit a complete inhibition of high-affinity EGFR ligand–induced signaling and proliferation

The observed broad range of inhibition could be simply due to the higher binding affinity of GC1118 to EGFR compared with

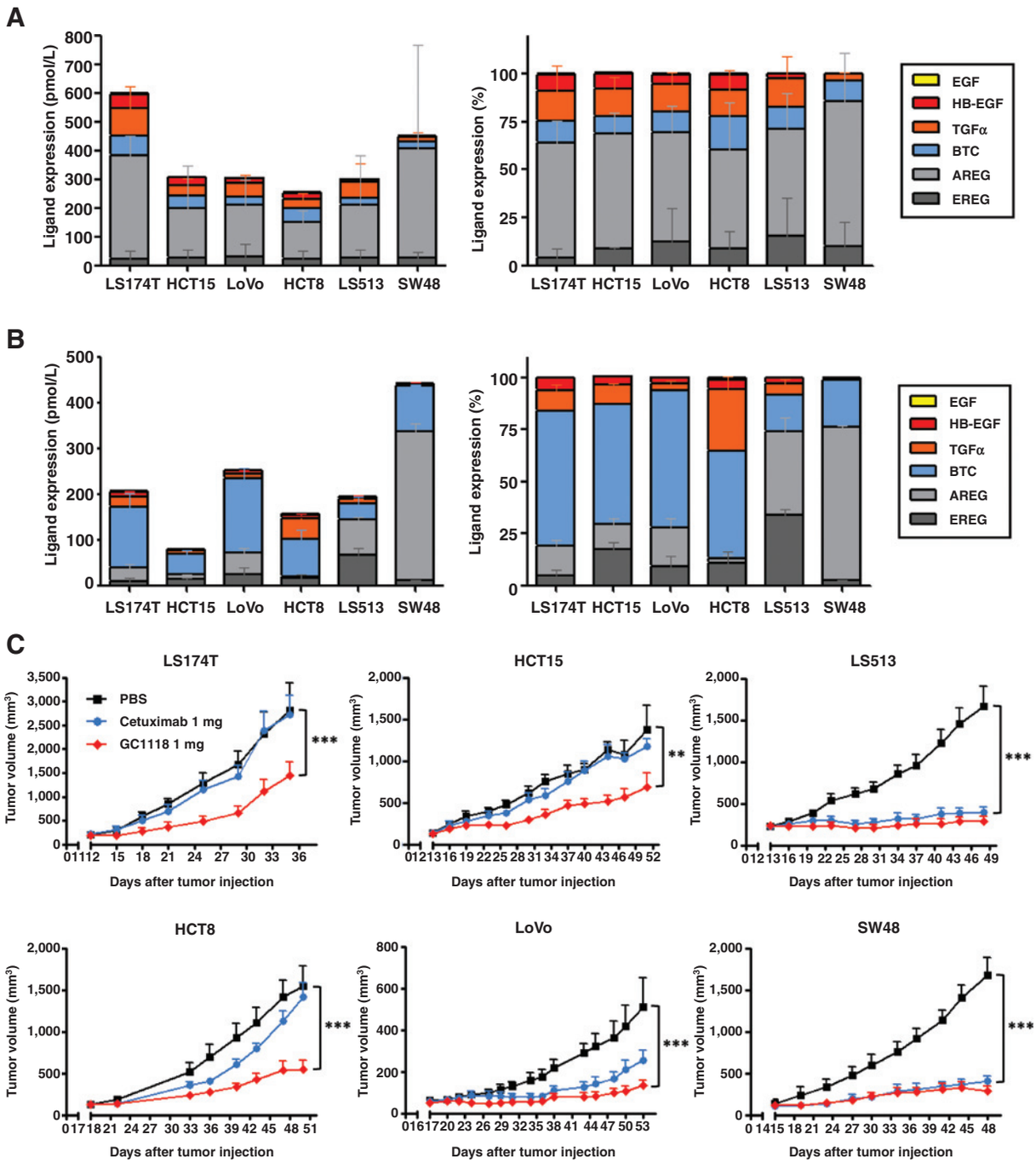

Figure 5.
GC1118 shows a superior tumor-inhibitory effect on colorectal cancer xenograft models harboring greater EGFR high-affinity ligand secretion. A, the basal secretory levels of EGFR ligands by the indicated cell lines were measured from the *in vitro* 72-hour cultured cell medium. B, the basal levels of EGFR ligands expressed by the indicated cell lines were measured from the tumor xenografts. C, athymic nu/nu mice were injected subcutaneously with HCT8, LoVo, HCT15, LS174T, LS513, and SW48 cells. GC1118 or cetuximab was administered intraperitoneally at 1 mg/mouse. $n = 6$ animals/group. The data are plotted as the mean values ±SD. Two-way ANOVA; **, $P < 0.01$, and ***, $P < 0.001$, compared with the PBS group.

cetuximab. To eliminate this possibility, we compared the inhibitory effect of GC1118 with panitumumab ($K_D = 0.05$ nmol/L), which was reported to have a one log higher binding affinity compared with cetuximab but with a binding epitope similar to cetuximab (40). The weak inhibitory activity of panitumumab towards the high-affinity ligands was more pronounced in the EGFR signaling downstream effectors such as Erk and Akt (Fig. 4A and Fig. 6A). Panitumumab at a dose of 50 μg/mL inhibited

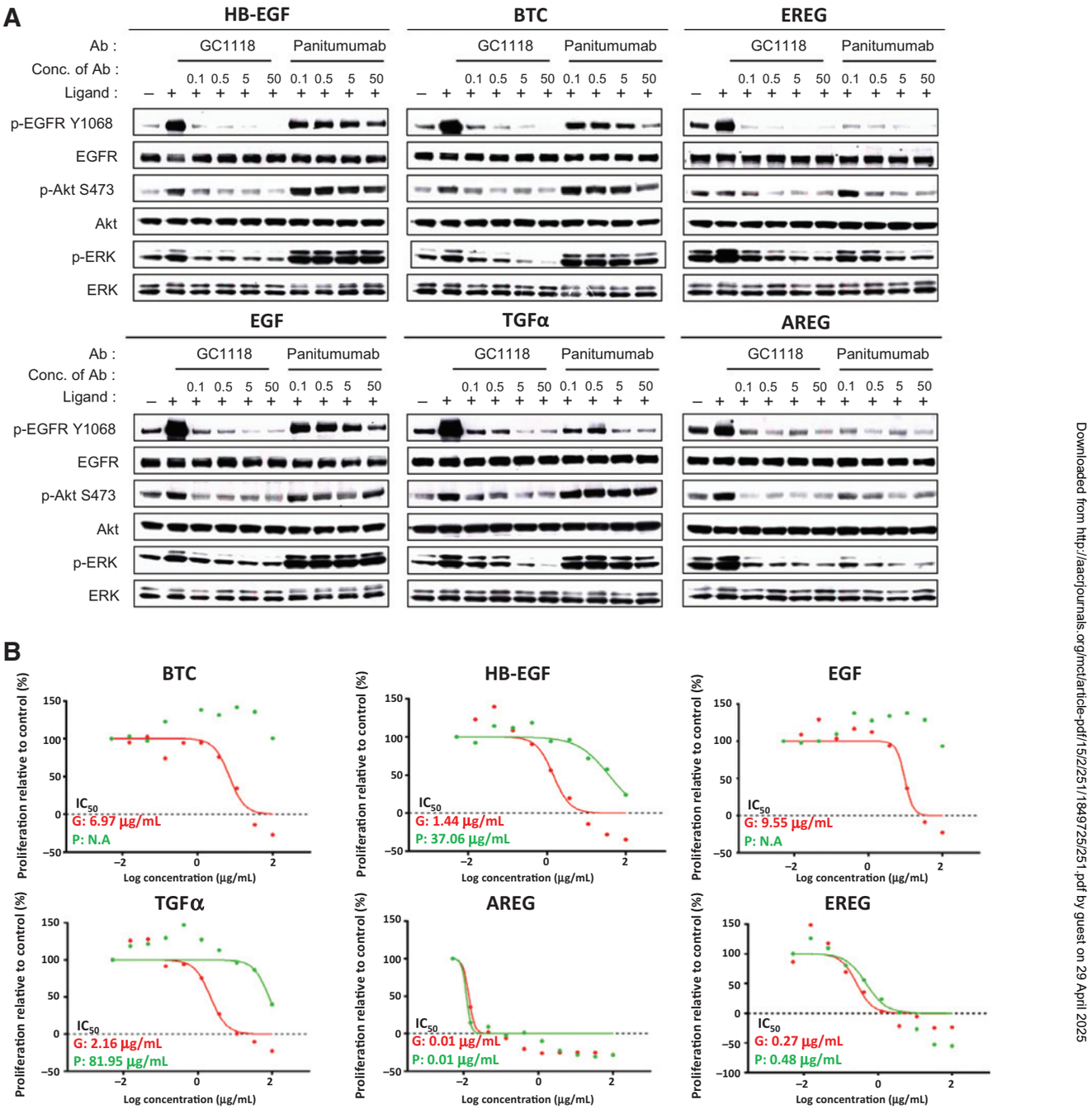

Figure 6.
Panitumumab exhibits limited inhibitory activity on high-affinity ligand-induced EGFR signaling and proliferation. A, HCT8 cells were serum starved for 18 hours, treated with 0.1 to 50 μg/mL GC1118 or panitumumab for 2 hours, and stimulated with EGFR ligands (EGF, HB-EGF, BTC, and TGFα, 250 ng/mL; AREG, 300 ng/mL; EREG, 500 ng/mL). pEGFR, pAKT, pERK, EGFR, AKT, or ERK expression levels were analyzed by Western blotting. B, HCT8 cells were serum starved for 18 hours, treated with ligands (EGF and HB-EGF, 50 ng/mL; BTC, 100 ng/mL; TGFα, 200 ng/mL; AREG and EREG, 300 ng/mL) and various amounts of GC1118 or panitumumab (0.005–100 μg/mL in high-affinity ligand-induced proliferation, 5 pg/mL–10 μg/mL in low-affinity ligand-induced proliferation) for three days. Cell proliferation was analyzed using an MTS assay. Red lines represent GC1118-treated cells and green lines indicate panitumumab-treated cells.

HB-EGF, BTC, TGFα, and EGF-induced phosphorylation of EGFR but not of Erk and Akt (Fig. 6A). This result indicates that panitumumab failed to completely inhibit EGFR signaling (Fig. 6A). A similar trend of inhibition was also observed in EGFR ligand–driven cell proliferation, where the inhibitory activities of panitumumab were restricted to only low-affinity EGFR ligands (Fig. 6B).

Discussion

In this study, we report a novel anti-EGFR antibody, GC1118, which exhibits a different binding affinity, binding epitope, and ligand-competitive activity from other EGFR antibodies. While cetuximab and panitumumab showed inhibitory activities that were limited to low-affinity ligands, GC1118 showed a potent inhibition of a broad range of ligands, ligand-induced EGFR signaling, and proliferation (Figs. 4–6). Because the expression of high-affinity ligands such as HB-EGF and TGFα has been implicated in various cancers (15–18) and in the lack of response or acquired resistance to cetuximab (13, 14), our results indicate that GC1118 may have a broad cancer patient pool including those patients progressed after treatment with current EGFR-targeted therapeutics. On the basis of these promising preclinical results, a phase I clinical trial is under study (ClinicalTrials.gov.Identifier: NCT02352571).

The superior inhibitory activity of GC1118 against high-affinity EGFR ligands appears to arise from a unique binding epitope as well as a high EGFR-binding affinity. Cetuximab, with a dissociation constant (K_D) of 10^{-9} mol/L, was displaced from EGFR by excess amounts of high-affinity ligands (Fig. 3) and failed to inhibit high-affinity ligand-induced signaling. Panitumumab, with a presumably higher binding affinity than cetuximab, also showed a limited suppressive effect on high-affinity ligands (Fig. 6). Panitumumab was reported to have the highest binding affinity to EGFR among the marketed EGFR antibodies (40) and appears to have a higher or comparable binding affinity to GC1118. Overall, these results strongly suggest that the binding epitope is one of the major factors leading to unique ligand-inhibitory activities of GC1118.

The crystal structure of the Fab fragment of GC1118 in complex with sEGFR identified a tethered structure of EGFR. This finding indicates that the binding of GC1118 to EGFR blocks the binding of other ligands and keeps EGFR in a tethered form. Both GC1118 and cetuximab bind to domain III of EGFR, but their binding regions are quite different. The binding epitope of GC1118 is located in a discrete area that mostly covers R353-H359, including D355 and F357, which are critical for EGF binding. The binding epitopes of cetuximab are widely dispersed and mostly overlap with Q384-S468 of the EGF-binding sites (34). According to a mutation analysis, a mutation at D355/F357 did not disturb the binding intensity of cetuximab toward EGFR as much as it did on the EGF–EGFR interaction, suggesting that the interactions with D355, F357, and Q384 are not the major contributors for the cetuximab–EGFR interaction (34). The critical residues of EGFR for EGF binding were reported to be D355 and F357 interacting with EGF R41 and EGF Y13, respectively, and the residues that constitute the hydrophobic pocket (L382, I438, F412) accommodating EGF L47 (37). Because a drastic decrease of the binding affinity of EGF to EGFR was observed by mutations at site 2 compared with site 3, it is conceivable that targeting site 2 would be more efficient in blocking the EGF–EGFR interaction. The binding sites of panitumumab are adjacent to and partially overlap with those of cetuximab, which are located mostly on the C-terminal regions of domain III, and this situation might explain the similar inhibitory pattern of panitumumab to cetuximab (41).

The superior inhibitory effect of GC1118 on high-affinity EGFR ligands forecasts therapeutic implications of GC1118 for a broader range of cancer patients than other current EGFR therapeutics. Gene expression analysis from a clinical study suggests that cetuximab has limited disease control in colorectal cancer patients with elevated levels of TGFα, which accounts for approximately one-third of the colorectal cancer patients tested (13). It is plausible that those patients having higher expression of TGFα and not responding to cetuximab would benefit from GC1118. EGFR and high-affinity EGFR ligands have been implicated in the generation and activation of tumor vasculature (42–44). Therefore, we expect that the tumor-inhibitory activities of GC1118 are not restricted to tumor proliferation only but also extend to influence the crosstalk of tumors with stromal factors leading to migration and invasion.

K-Ras mutation is a negative predictive marker of the response to EGFR-targeted antibody therapeutics based on many clinical trials, where patients with K-Ras mutation had no benefit from additional EGFR-targeted antibody therapy in terms of response rate, progression-free survival, and overall survival compared with the standard chemotherapy therapy group (45). More than half of the mCRC patients with wild-type K-Ras, however, do not respond to EGFR-targeted therapies, and this result was later reported to be due to mutations or loss of a gene in the downstream K-Ras signaling molecules, such as B-Raf, PIK3CA, and PTEN. Khambata and colleagues and Jacob and colleagues reported that, in K-Ras wild-type mCRC patients, the gene expression levels of EGFR ligands AREG and EREG were associated with disease control upon treatment with cetuximab (12, 46). This finding suggests the existence of subgroups of mCRC patients whose tumors are dependent on the ligand-mediated EGFR circuit for survival and tumor progression. On the other hand, disease control with cetuximab did not correlate well with the mRNA expression levels of other known EGFR ligands, such as EGF, TGFα, BTC, and HB-EGF (13). With regard to high-affinity ligands, these data are in line with our observation of the inefficient inhibitory efficacy of cetuximab on high-affinity ligand-induced signaling and proliferation and supports the notion that GC1118 could provide another therapeutic option to those patients who failed in current EGFR-targeted therapeutics.

Disclosure of Potential Conflicts of Interest

No potential conflicts of interest were disclosed.

Authors' Contributions

Conception and design: Y. Lim, M. Hur, T.W. Park, K. Lee, K.H. Chang, S.-H. Kim, Y. Yoon, H.-S. Cho, J. Won

Development of methodology: M. Hur, K. Lee, S.-H. Kim, J. Won

Acquisition of data (provided animals, acquired and managed patients, provided facilities, etc.): Y. Lim, J. Yoo, M.-S. Kim, S.-N. Lee, K. Lee, Y. Kang, K.-W. Hong, Y.-G. Kim, H. Yang, J. Won

Analysis and interpretation of data (e.g., statistical analysis, biostatistics, computational analysis): Y. Lim, J. Yoo, M. Hur, E.H. Lee, H.-S. Hur, J.-C. Lee, S.-N. Lee, T.W. Park, K. Lee, K.H. Chang, Y. Yoon, H.-S. Cho, J. Won

Writing, review, and/or revision of the manuscript: Y. Lim, J. Yoo, M.-S. Kim, H.-S. Cho, J. Won

Administrative, technical, or material support (i.e., reporting or organizing data, constructing databases): J. Yoo, M. Hur, E.H. Lee, S.-N. Lee, K. Lee, K. Kim, K.-W. Hong, Y. Yoon, D.G. Kim, H.-S. Cho, J. Won

Study supervision: K.H. Chang, S.-H. Kim, Y. Yoon, D.-H. Nam, H.-S. Cho, J. Won

Acknowledgments

The authors thank the staff scientists at the BL-17A beamline of the Photon Factory and the beamline 5C and 7A of the Pohang Light Source for data collection. The authors also thank Dr. Sujeong Kim for the critical review.

Grant Support

This work was supported by grants of the Korea Healthcare technology R&D project, Ministry for Health & Welfare Affairs, Republic of Korea (HI14C3418; to J. Won, Y. Lim, M. Hur, J.-C. Lee, S.-N. Lee, T.W. Park, Y. Yoon, D.-H. Nam, H. Yang, and D.G. Kim), A080320 (to H.-S. Cho, J. Yoo, K. Kim, and Y. Kang). All authors received the grant from the Green Cross Corp., Republic of Korea. This work was also funded by the Mid-career Researcher Program through a NRF grant, the Korea government (MEST; no. 2009-0073145, 2009-0084897, NRF-2012R1A2A2A01012830; to H.S. Cho, J. Yoo, K. Kim, and Y. Kang).

The costs of publication of this article were defrayed in part by the payment of page charges. This article must therefore be hereby marked *advertisement* in accordance with 18 U.S.C. Section 1734 solely to indicate this fact.

Received August 14, 2015; revised November 9, 2015; accepted November 12, 2015; published OnlineFirst November 19, 2015.

References

1. Holbro T, Hynes NE. ErbB receptors: directing key signaling networks throughout life. Annu Rev Pharmacol Toxicol 2004;44:195–217.
2. Arteaga CL. Overview of epidermal growth factor receptor biology and its role as a therapeutic target in human neoplasia. Semin Oncol 2002;29:3–9.
3. Rocha-Lima CM, Soares HP, Raez LE, Singal R. EGFR targeting of solid tumors. Cancer Contr 2007;14:295–304.
4. Mendelsohn J, Baselga J. Status of epidermal growth factor receptor antagonists in the biology and treatment of cancer. J Clin Oncol 2003;21: 2787–99.
5. Yotsumoto F, Sanui A, Fukami T, Shirota K, Horiuchi S, Tsujioka H, et al. Efficacy of ligand-based targeting for the EGF system in cancer. Anticancer Res 2009;29:4879–86.
6. Sanders JM, Wampole ME, Thakur ML, Wickstrom E. Molecular determinants of epidermal growth factor binding: a molecular dynamics study. PLoS One 2013;8:e54136.
7. Jones JT, Akita RW, Sliwkowski MX. Binding specificities and affinities of egf domains for ErbB receptors. FEBS Lett 1999;447:227–31.
8. Wilson KJ, Mill C, Lambert S, Buchman J, Wilson TR, Hernandez-Gordillo V, et al. EGFR ligands exhibit functional differences in models of paracrine and autocrine signaling. Growth Factors 2012;30:107–16.
9. Roepstorff K, Grandal MV, Henriksen L, Knudsen SL, Lerdrup M, Grøvdal L, et al. Differential effects of EGFR ligands on endocytic sorting of the receptor. Traffic 2009;10:1115–27.
10. Sorkin A, Goh LK. Endocytosis and intracellular trafficking of ErbBs. Exp Cell Res 2009;315:683–96.
11. Yotsumoto F, Yagi H, Suzuki SO, Oki E, Tsujioka H, Hachisuga T, et al. Validation of HB-EGF and amphiregulin as targets for human cancer therapy. Biochem Biophysi Res Comm 2008;365:555–61.
12. Khambata-Ford S, Garrett CR, Meropol NJ, Basik M, Harbison CT, Wu S, et al. Expression of epiregulin and amphiregulin and K-ras mutation status predict disease control in metastatic colorectal cancer patients treated with cetuximab. J Clin Oncol 2007;25:3230–7.
13. Tabernero J, Cervantes A, Rivera F, Martinelli E, Rojo F, Heydebreck A, et al. Pharmacogenomic and pharmacoproteomic studies of cetuximab in metastatic colorectal cancer: biomarker analysis of a phase I dose-escalation study. J Clin Oncol 2010;28:1181–9.
14. Troiani T, Martinelli E, Napolitano S, Vitagliano D, Ciuffreda LP, Costantino S, et al. Increased TGF-alpha as a mechanism of acquired resistance to the anti-EGFR inhibitor cetuximab through EGFR-MET interaction and activation of MET signaling in colon cancer cells. Clin Cancer Res 2013; 19:6751–65.
15. Tanaka Y, Miyamoto S, Suzuki SO, Oki E, Yagi H, Sonoda K, et al. Clinical significance of heparin-binding epidermal growth factor-like growth factor and a disintegrin and metalloprotease 17 expression in human ovarian cancer. Clin Cancer Res 2005;11:4783–92.
16. Miyamoto S, Hirata M, Yamazaki A, Kageyama T, Hasuwa H, Mizushima H, et al. Heparin-binding EGF-like growth factor is a promising target for ovarian cancer therapy. Cancer Res 2004;64:5720–7.
17. Olsen DA, Bechmann T, Østergaard B, Wamberg PA, Jakobsen EH, Brandslund I. Increased concentrations of growth factors and activation of the EGFR system in breast cancer. Clin Chem Lab Med 2012;50: 1809–18.
18. Rusch V, Klimstra D, Venkatraman E, Pisters PW, Langenfeld J, Dmitrovsky E. Overexpression of the epidermal growth factor receptor and its ligand transforming growth factor alpha is frequent in resectable non-small cell lung cancer but does not predict tumor progression. Clin Cancer Res 1997;3:515–22.
19. Burgess AW, Cho HS, Eigenbrot C, Ferguson KM, Garrett TP, Leahy DJ, et al. An open-and-shut case? Recent insights into the activation of EGF/ErbB receptors. Mol Cell 2003;12:541–52.
20. Zhang X, Gureasko J, Shen K, Cole PA, Kuriyan J. An allosteric mechanism for activation of the kinase domain of epidermal growth factor receptor. Cell 2006;125:1137–49.
21. Ogiso H, Ishitani R, Nureki O, Fukai S, Yamanaka M, Kim JH, et al. Crystal structure of the complex of human epidermal growth factor and receptor extracellular domains. Cell 2002;110:775–87.
22. Cho HS, Leahy DJ. Structure of the extracellular region of HER3 reveals an interdomain tether. Science 2002;297:1330–3.
23. Mendelsohn J. Targeting the epidermal growth factor receptor for cancer therapy. J Clin Oncol 2002;20:1S–13S.
24. Ciardiello F, Tortora G. EGFR antagonists in cancer treatment. N Engl J Med 2008;358:1160–74.
25. Dienstmann R, Patnaik A, Garcia-Carbonero R, Cervantes A, Benavent M, Roselló S, et al. Safety and activity of the first-in-class sym004 anti-EGFR antibody mixture in patients with refractory colorectal cancer. Cancer Discov 2015;5:598–609.
26. Kearns JD, Bukhalid R, Sevecka M, Tan G, Gerami-Moayed N, Werner SL, et al. Enhanced targeting of the EGFR network with MM-151, an oligoclonal anti-EGFR antibody therapeutic. Mol Cancer Ther 2015;14: 1625–36
27. Otwinowski Z, Minor W. Processing of X-ray diffraction data collected in oscillation mode. Method Enzymol 1997;276:307–26.
28. Vagin AA, Isupov MN. Spherically averaged phased translation function and its application to the search for molecules and fragments in electron-density maps. Acta Crystallogr D Biol Crystallogr 2001;57: 1451–6.
29. Winn MD, Ballard CC, Cowtan KD, Dodson EJ, Emsley P, Evans PR, et al. Overview of the CCP4 suite and current developments. Acta Crystallogr D Biol Crystallogr 2011;67:235–42.
30. Emsley P, Lohkamp B, Scott WG, Cowtan K. Features and development of Coot. Acta Crystallogr D Biol Crystallogr 2010;66:486–501.
31. Murshudov GN, Vagin AA, Dodson EJ. Refinement of macromolecular structures by the maximum-likelihood method. Acta Crystallogr D Biol Crystallogr 1997;53:240–55.
32. Chang KH, Kim MS, Hong GW, Shin YN, Kim SH. Conversion of a murine monoclonal antibody A13 targeting epidermal growth factor receptor to a human monoclonal antibody by guided selection. Exp Mol Med 2012;44: 52–9.
33. Chang KH, Kim MS, Hong GW, Seo MS, Shin YN, Kim SH. Affinity maturation of an epidermal growth factor receptor targeting human monoclonal antibody ER414 by CDR mutation. Immune Netw 2012;12: 155–64.
34. Li S, Schmitz KR, Jeffrey PD, Wiltzius JJ, Kussie P, Ferguson KM. Structural basis for inhibition of the epidermal growth factor receptor by cetuximab. Cancer Cell 2005;7:301–11.
35. Schmiedel J, Blaukat A, Li S, Knöchel T, Ferguson KM. Matuzumab binding to EGFR prevents the conformational rearrangement required for dimerization. Cancer Cell 2008;13:365–73.36.
36. Engler DA, Campion SR, Hauser MR, Cook JS, Niyogi SK. Critical functional requirement for the Guanidinium group of the arginine 41 side

chain of human epidermal growth factor as revealed by mutagenic inactivation and chemical reactivation. J Biol Chem 1992;267:2274–81.
37. Tadaki DK, Niyogi SK. The functional importance of hydrophobicity of the tyrosine at Position 13 of human epidermal growth factor in receptor binding. J Biol Chem 1993;268:10114–9.
38. Garrett TP, McKern NM, Lou M, Elleman TC, Adams TE, Lovrecz GO. Crystal structure of a truncated epidermal growth factor receptor extracellular domain bound to transforming growth factor alpha. Cell 2002;110: 763–73.
39. Rojas M, Yao S, Lin YZ. Controlling epidermal growth factor (EGF)-stimulated Ras activation in intact cells by a cell-permeable peptide mimicking phosphorylated EGF receptor. J Biol Chem 1996;271: 27456–61.
40. Yang XD, Jia XC, Corvalan JR, Wang P, Davis CG. Development of ABX-EGF, a fully human anti-EGF receptor monoclonal antibody, for cancer therapy. Crit Rev Oncol Hematol 2001;38:17–23.
41. Voigt M, Braig F, Göthel M, Schulte A, Lamszus K, Bokemeyer C. Functional dissection of the epidermal growth factor receptor epitopes targeted by panitumumab and cetuximab. Neoplasia 2012;14:1023–31.
42. Yokoi K, Thaker PH, Yazici S, Rebhun RR, Nam DH, He J, et al. Dual inhibition of epidermal growth factor receptor and vascular endothelial growth factor receptor phosphorylation by AEE788 reduces growth and metastasis of human colon carcinoma in an orthotopic nude mouse model. Cancer Res 2005;65:3716–25.
43. Kuwai T, Nakamura T, Sasaki T, Kim SJ, Fan D, Villares GJ, et al. Phosphorylated epidermal growth factor receptor on tumor-associated endothelial cells is a primary target for therapy with tyrosine kinase inhibitors. Neoplasia 2008;10:489–500.
44. Sato S, Drake AW, Tsuji I, Fan J. A potent anti-HB-EGF monoclonal antibody inhibits cancer cell proliferation and multiple angiogenic activities of HB-EGF. PLoS One 2012;7:e51964.
45. Normanno N, Tejpar S, Morgillo F, Luca AD, Cutsem EV, Ciardiello F. Implications for KRAS status and EGFR-targeted therapies in metastatic CRC. Nat Rev Clin Oncol 2009;6:519–27.
46. Jacobs B, Roock WD, Piessevaux H, Oirbeek R, Biesmans B, Schutter J. Amphiregulin and epiregulin mRNA expression in primary tumors predicts outcome in metastatic colorectal cancer treated with cetuximab. J Clin Oncol 2009;27:5068–74.